Hindawi
Advances in Civil Engineering
Volume 2021, Article ID 5533879, 11 pages
https://doi.org/10.1155/2021/5533879

Research Article

Deflection Laws of Gas Drainage Boreholes in Interbedded Soft and Hard Seams: A Case Study at Xinzheng Coal Mine, China

Xiaoyan Sun,[1] Zhiheng Cheng,[2] Liang Chen,[2] Zhenhua Li,[3] Hongbing Wang,[4] and Shuaifeng Yin[2]

[1]*Chengdu University of Technology, Chengdu, Sichuan 610051, China*
[2]*School of Safety Engineering, North China Institute of Science and Technology, Beijing 101601, China*
[3]*School of Energy Science and Engineering, Henan Polytechnic University, Jiaozuo, Henan 454000, China*
[4]*School of Civil and Resource Engineering, State Key Laboratory of High-Efficiency Mining and Safety of Metal Mine, Ministry of Education, University of Science and Technology Beijing, Beijing, China*

Correspondence should be addressed to Zhiheng Cheng; an958158@163.com

Received 10 February 2021; Revised 8 April 2021; Accepted 8 July 2021; Published 9 September 2021

Academic Editor: Jian Ji

Coal and gas outbursts can lead to serious disasters in coal mines. The drilling of boreholes to predrain the gas is an effective measure for preventing such accidents. However, due to the complexity of the geological situation, the drilling trajectory often deviates from the design trajectory, resulting in poor gas extraction. To solve the problem of gas drainage borehole deflection, an analytic hierarchy process (AHP) model is established based on geological factors, technical factors, and human factors. The AHP model is used to rank the weights of various influencing factors, and the analysis is combined with a drilling model and engineering examples. Finally, the results show that soft and hard interlayers are the most important factors affecting the deflection of the borehole. The rock drilling model is mainly affected by the formation forces. The regularity of the change in the azimuth angle during drilling is not obvious when the angle of the encountered layer is less than some critical value. When the borehole is skewed downward, the deflection angle ranges from 0 to 4°, and the deflection of the borehole occurs mainly at the interface of the rock layers. When the angle of the encountered layer is greater than the critical value, the borehole is skewed upward, with a deflection angle of 0–6°, and the deflection occurs at the rock interface. The trajectory curve obtained by theoretical predictions from field data is found to be consistent with that of an actual project.

1. Introduction

Coal and gas outbursts can result in serious disasters in coal mines [1–5]. In response to this problem, many scholars have conducted research related to rock mechanics and gas flow [6–13]. At present, the use of drilling boreholes to predrain coal-seam gas is a common and effective measure for preventing such accidents [14, 15]. However, when drilling in soft and outburst-prone coal seams, problems such as buried drilling, injection boreholes, and stuck drills are prone to occur, and the actual drilling trajectory often deviates from the designed trajectory [16, 17]. This leads to unqualified gas control drilling, which not only wastes construction time, manpower, materials, and financial resources but also seriously affects the gas drainage effect. Therefore, it is necessary to study the deflection law of gas drilling in soft outburst-prone coal seams [18, 19].

Aiming at the problem of borehole deflection, Gao et al. [20] analyzed the lateral penetration ability of the drill bit, which is different from its axial penetration ability. The inclination angle and lateral force of the drill bit were determined based on a weighted residual method. Wang et al. [21] obtained the contact characteristics between boreholes and calculated the dynamic lateral force on the drill bit, which led to a deviation control mechanism based on the motion stability and dynamic lateral force. Gao and Zheng [22] studied the changes in the formation characteristics of the bottom borehole in the process of air drilling. A large

anisotropy index in air drilling was found to lead to more serious well deviation, and an increase in the penetration depth of the bit teeth aggravates this deviation. Morin and Wilkens [23] reported that the bit tends to be perpendicular to the fracture strike in the drilling process and used the deviation logarithm to describe the trajectory of the borehole in three-dimensional space. Chen et al. [24] proposed a bit formation wellbore model for a nonlinear coupled bottom borehole assembly under full screw drilling. Liu et al. [25] established a linear elastic model of borehole collapse failure based on pore fluid seepage and obtained the attenuation law for the soft coal seam collapse pressure with gas seepage; the basic mechanical parameters of the coal seam and fluid seepage and the space of the borehole trajectory were also analyzed. The influence of factors such as the azimuth angle of drilling on the borehole collapse provides theoretical support for soft rock formations and the deflection of boreholes in coal seams.

Although the abovementioned studies covered research on the law and control of borehole deflection, the resulting deflection laws are somewhat vague, making a qualitative and quantitative analysis of the deflection law impossible. There have been few studies on borehole deflection in gas treatment, so this work focuses on solving the problem of the blind area of gas drainage and the inability to achieve effective gas drainage. The deflection law and main influencing factors of gas treatment boreholes are analyzed, and the borehole deflection trajectory equation is determined. Additionally, the relationship between the magnitude of deflection and the main influencing factors is identified. This paper describes the use of an analytic hierarchy process (AHP) model to sort the weights of the influencing factors and analyzes the drilling model and engineering examples. The deflection law is then derived, allowing effective predictions of coal-seam gas to be realized. Pumping provides a strong guarantee of preventing the occurrence of coal and gas outbursts and gas overruns and ensures a certain basis for the study and control of borehole deflection in high-gas mines and coal/gas outburst mines.

2. Factors Affecting Borehole Deflection

A literature review and field investigations suggest that the main factors influencing borehole deflection during natural gas extraction are drilling depth, lithology, rock inclination, drilling speed, drilling rig performance, and supporting facilities. These influencing factors can be divided into three aspects: geological factors, technological factors, and human factors.

2.1. Geological Factors. Geological factors are the objective causes of borehole deflection. The main geological factors are rock anisotropy, weak interlayers, and rock angles:

(i) *Rock Anisotropy*. The rock anisotropy has an important influence on the choice of drilling direction and method. In other words, the degree of rock anisotropy determines the techniques and technologies used for drilling in the formation.

(ii) *Weak Interlayers*. The principle that soft and hard interlayers affect the drilling trajectory is that when drilling through a hard rock formation at an acute angle, the different pressure resistance of the soft rock and hard rock causes the trajectory of drilling to curve along the direction perpendicular to the rock formation. When passing into soft rock from hard rock, the axis of the drilling tool in the borehole will deviate from the normal line of the rock layer. However, the lithology of the borehole wall of the hard rock above is relatively hard, which limits the drilling tool in the borehole. The final result is that the trajectory of the borehole will basically be offset in the original direction; when the borehole passes into hard rock from soft rock and then through the hard rock, the final result is still an offset along the route of the hard rock facet.

(iii) *Rock Angles*. In the stratum where gneiss is developed and the rock angle is acute, the drilling trajectory will bend in the direction perpendicular to the stratum angle.

2.2. Technical Factors. Technical factors influence the whole lifecycle of the drilling process. The main technical factors are equipment installation, drilling tool structure, and drilling tool weight:

(i) *Equipment Installation*. The uneven foundation of drilling sites and the restricted space mean that the borehole inclination is often less than required. Additionally, the magnetism of the field equipment will interfere with the compass used to determine the borehole position. These factors will affect the drilling trajectory. When the equipment is not adequately stabilized, the equipment will swing back and forth during the drilling process, causing deviations in the drilling trajectory and producing serious safety hazards.

(ii) *Drilling Tool Structure*. The influence of the drilling tool structure on the drilling trajectory is mainly reflected in the drilling tool length, borehole wall clearance, and drilling tool rigidity. The size of the borehole wall clearance and the length of the drill tool determine the deflection angle of the drill tool in the borehole. When the borehole wall gap increases or the length of the drill tool decreases, the deflection angle of the drill tool in the borehole will increase. A more rigid drilling tool will undergo less deformation under the action of axial pressure, thus reducing the impact on the drilling trajectory.

(iii) *Self-Weight of Drilling Tool*. In the process of directional drilling, the main drilling tools in the borehole include the drill bit, screw motor, nonmagnetic lower tube, probe pipe, nonmagnetic upper tube, and drill pipe. As the borehole depth increases, the weight of the drill pipe becomes heavier and the impact on the trajectory of the borehole becomes greater.

2.3. Human Factors. Human factors determine the efficiency of drilling. The main human factors are the drilling method, drilling procedure parameters, weight on bit (WOB) selection, and drilling speed selection:

(i) *Drilling Method*. There are many construction methods for underground drilling in coal mines. Different drilling methods have different characteristics in terms of the broken rock and borehole wall gaps, which ultimately affect the deviation of the drilling trajectory. The current drilling methods include percussion drilling, rotary drilling, percussive rotary drilling, vibration drilling, and hybrid drilling. Adopting reasonable drilling methods for the site conditions can effectively control the drilling trajectory while improving the drilling efficiency.

(ii) *Drilling Procedure Parameters*. The influence of drilling parameters on the drilling trajectory is mainly reflected in the coordination of the drilling pressure and the drilling speed. If the drilling pressure of the drilling rig is too large, it will cause the drilling tool in the borehole to bend, and the drill bit will be biased to the side of the borehole wall. The optimized processing and reasonable coordination of the drilling pressure and the drilling speed can effectively reduce the deviation of the drilling trajectory.

(iii) *WOB Selection*. When the drilling pressure is too high, the cutting volume will be excessive and the cutting tool will become completely buried in the rock formation. At the same time, the cooling and powder discharge conditions at the bottom of the drill hole deteriorate, and the wear on the bit increases, making the drilling less effective. The choice of drill weight depends on the rock abrasiveness, drillability, particle size, quantity, grade, bottom lip area of the diamond bit, and other factors.

(iv) *Drilling Speed Selection*. Rotation speed is the main aspect affecting drilling efficiency. Strict control of the drilling speed of the drill pipe so as to achieve more grinding and less advancement improves the qualification rate of drilling. For softer and less abrasive rocks, the drilling speed can be increased by increasing the rotation speed; for hard and abrasive rocks, too high a rotation speed not only reduces the drilling effect but also harms the drilling advancement process. When selecting the drilling speed, the drill bit type, flushing fluid (with or without lubricant), ability of the drilling rig, strength of the drill string, and cutting tool should also be considered, and the appropriate speed should be determined through comprehensive analysis.

3. AHP Model

AHP [26, 27] is an effective method for transforming semiqualitative and semiquantitative problems into quantitative systems. It is applicable to systems with complex evaluation structures. The basic principle and main steps of AHP are as follows: first, according to the characteristics of the actual scenario, the problem is decomposed layer by layer, and the AHP structure model of the overall target and the hierarchical target is established; second, the judgment matrix from the lower-level target to the higher-level target is constructed, and the evaluation indexes of the same level are compared in pairs to calculate the weight value relative to the higher-level target (hierarchical single ranking table). Finally, the results are combined with the total target weight value to obtain the total ranking table.

3.1. Establishment of AHP Model. To determine the deflection from internal and external causes and considering the factor of quantitative maneuverability, a selection of geological factors (U_1), technology factors (U_2), and human factors (U_3) were incorporated into the AHP model. Specifically, the proposed AHP model considers the rock anisotropy (U_{11}), hard and soft interbed layers (U_{12}), angle of bedding (U_{13}), equipment installation (U_{21}), drilling tool structure (U_{22}), weight of drill tool (U_{23}), drilling method (U_{31}), drilling parameters (U_{32}), weight on bit (U_{33}), and drilling rate selection (U_{34}), a total of 10 impact factors. The structure of the proposed AHP model is shown in Figure 1.

3.2. Determination of the Weight. According to the AHP model described above, judgment matrices for the second- and third-level targets were constructed using the 1–9 scale method. Combined with practical experience, this allowed the weight values of each impact factor in each judgment matrix to be calculated (Tables 1–4). Finally, the weight values of the third- and second-level targets were multiplied from the bottom, and the results were further synthesized with the total target to obtain the total weight ranking of each impact factor [28, 29].

(i) *Determine the Judgment Matrix of Each Level*. On the basis of each criterion layer, the result table from comparing each pair of elements was established, and the judgment matrices of each layer versus the next were obtained from Tables 1–4. The results are as follows:

(a) Judgment matrix A_z of the criterion layer to the target layer Z [30]:

$$A_Z = \begin{bmatrix} 1 & 2 & 5 \\ \frac{1}{2} & 1 & 2 \\ \frac{1}{5} & \frac{1}{2} & 1 \end{bmatrix}. \quad (1)$$

(b) Judgment matrix A_{U1} between indicator layer and criterion layer Z:

$$A_{U1} = \begin{bmatrix} 1 & \frac{1}{6} & \frac{1}{2} \\ 6 & 1 & 3 \\ 2 & \frac{1}{3} & 1 \end{bmatrix}. \quad (2)$$

(c) Judgment matrix A_{U2} between indicator layer and criterion layer U_2:

$$A_{U2} = \begin{bmatrix} 1 & \frac{1}{2} & 1 \\ 2 & 1 & 1 \\ 1 & 1 & 1 \end{bmatrix}. \quad (3)$$

(d) Judgment matrix AU_3 between indicator layer and criterion layer U_3:

$$A_{U3} = \begin{bmatrix} 1 & 1 & \frac{1}{2} & \frac{1}{2} \\ 1 & 1 & \frac{1}{2} & \frac{1}{2} \\ 1 & 2 & 1 & 1 \\ 2 & 2 & 1 & 1 \end{bmatrix}. \quad (4)$$

(ii) *Calculate the Importance Ranking*. According to the judgment matrices, the eigenvector corresponding to the maximum eigenvalue can be calculated using the following equation, where P is the judgment matrix and the eigenvector W is normalized to form the order of importance of each evaluation factor, that is, the weight allocation:

$$PW = \lambda_{\max} W. \quad (5)$$

Using the square root method to solve this equation, we calculate the judgment matrix P for the product of each row of elements M and then calculate the cubic root W of M_i. The vector $W = (W_1, W_2, W_3)$ is normalized according to $W_i = W_i / [\sum_{i=1}^{2} W_i]$, and the resulting $W = (W_1, W_2, W_3)$ is the eigenvector. According to the above steps, the eigenvector of the judgment matrix A_z can be calculated as (0.606, 0.265, 0.129).

(iii) *Consistency Test*. To determine whether the weight distribution is reasonable, the consistency of the judgment matrix needs to be tested using the following expression:

$$\mathrm{CR} = \frac{\mathrm{CI}}{\mathrm{RI}}, \qquad \mathrm{CI} = \frac{(\lambda_{\max} - n)}{(n-1)}. \quad (6)$$

where CR is the consistency index value, CI is the random consistency ratio of the judgment matrix, RI is the average consistency index of the judgment matrix, and N is the order of the judgment matrix; the RI values of the judgment matrix, ordered from 1–9, are presented in Table 5.

The maximum eigenvalue of the judgment matrix is calculated and converted to

$$\lambda_{\max} = \sum_{i=1}^{3} \frac{(PW)_i}{nW_i} = \frac{1}{n} \sum_{i=1}^{3} \frac{(PW)_i}{W_i}, \quad (7)$$

where $(PW)_i$ represents the i-th element of PW, and the order of the judgment matrix is $n = 3$.

$$PW = \begin{pmatrix} (PW)_1 \\ (PW)_2 \\ (PW)_3 \end{pmatrix}. \quad (8)$$

The known data in Table 5 are substituted into equation (3) and the maximum eigenvalue is calculated; in this case, Max = 3.03. As shown in Table 6, RI = 0.58 and CR = 0.025 < 0.1. This indicates that the judgment matrix has satisfactory consistency, so each component of $W = (W_1, W_2, W_3)$ can be used as a weight coefficient. Similarly, the second-level weight set can be calculated: Max = 3.01, CR1 = 0.01 < 0.1, Max = 3.08, CR2 = 0.060 < 0.1, and Max = 4.06, CR3 = 0.02 < 0.1.

(iv) *Calculate the Composite Weight of Each Layer to the Target Layer*. The synthetic weight of each element to the target layer refers to the synthesis of the relative weight of each factor of each judgment matrix to the target layer (the topmost layer). This weight is calculated using a top-down method, that is, layer-by-layer synthesis. The composite weights and their total rankings are listed in Table 6.

(v) Overall ranking consistency ratio is as follows:

$$\mathrm{CR} = \frac{\sum_{i=1}^{3} W_i \mathrm{CI}_i}{\sum_{i=1}^{3} W_i \mathrm{RI}_i} = \frac{0.606 * 0.01 + 0.265 * 0.06 + 0.129 * 0.02}{0.606 * 0.58 + 0.265 * 0.58 + 0.129 * 1.12} = 0.026 < 0.1. \quad (9)$$

Thus, the total sorting results of the hierarchy meet the consistency requirement.

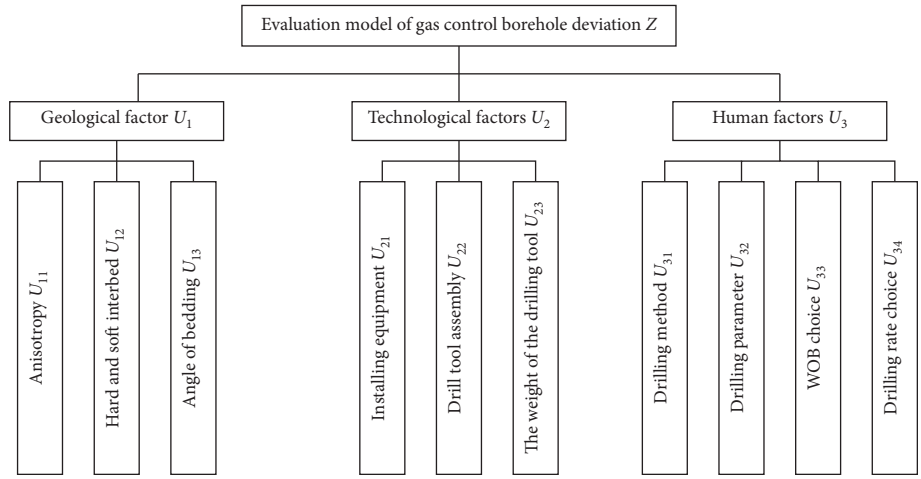

Figure 1: Hierarchical structure model of borehole deflection evaluation.

Table 1: Judgment matrix table Z.

Borehole deflection Z	U_1	U_2	U_3	Weight
U_1	1	2	5	0.606
U_2	1/2	1	2	0.265
U_3	1/5	1/2	1	0.129

4. Field Test

4.1. Overview of the Test Site. The 14205 working face of Xinzheng Coal and Electricity Co., Ltd., is a flat surface with a ground elevation of +134.9–+137.2 m. The working face elevation ranges from −152.0 m to −193.0 m, the working face slope is 187 m, the strike length is 668 m, and the coal seam inclination is 0–11°. The coal thickness is 0.5–12 m, and the bottom roadway is 12–15 m away from the coal seam. On-site surveys indicate that the mining area was mainly used in the initial stage of the drilling site, and a gas control borehole was drilled on the roadway wall at a later stage. The site layout is shown in Figure 2.

4.2. Test Results. A total of 421 sets of drilling inclination data from the bottom-draining roadway of site 14205 were collected. The changes in the top angle (θ) and azimuth angle (α) of each borehole section are summarized in Table 7. Due to the large amount of drilling data, not all of the statistics can be listed here. Note, however, that both the vertex angle and the azimuth angle change in 81.9% of cases; that is, deviation occurred in the majority of drilling processes .

(i) *Change in Azimuth*. Figure 3 shows the azimuth angle change diagram of boreholes 40–53. The general characteristics of the overall upper azimuth angle change are as follows. During the drilling process, the azimuth angle body exhibits an increasing trend. Half of the cases are skewed to the left with a deflection angle of 0–2°, and the other half are skewed to the right with a deflection angle of 0–1.7°, with an overall increasing trend.

(ii) *Inclination Angle Change*. According to the field survey data collected by the bottom alley roadway of site 14205, the main constituents of the drilling zone are limestone (*L*7 and *L*8), sandy mudstone, and a 2-1 coal seam. The *L*7 limestone with *L*8 limestone has the greatest strength, with a uniaxial compressive strength of around 62.0–62.3 MPa. The sandy mudstone is relatively weak, with a uniaxial compressive strength generally in the range of 19.0–42.3 MPa. Thus, at the bottom alley roadway of site 14205, drilling extraction from above will involve drilling through hard and soft interbed structures.

(a) *When the Angle of the Encountered Layer is Less Than the Critical Value*. Using the SPSS data platform to sort the field data, the critical angle was found to be 25–35°. Figure 4 shows that when the angle of the encountered layer is less than the critical value, the overall downward deflection of the borehole is between 0 and 4° and the overall offset is from 1 to 6.1 m (average of 3.0 m). When the angle of the encountered layer is less than the critical value, the offset in the vertical direction is larger in deeper boreholes. The vertical displacement tends to increase over the extent of the borehole, and so the borehole trajectory gradually moves away from the design trajectory (Figure 5).

The borehole trajectory deflection condition is compared with a geological model of the regional change corresponding to *L*8 limestone in Figure 6. The relatively soft sandy mudstone produces small deviations when drilling, whereas drilling through

Table 2: Judgment matrix table U_1.

Geological factors U_1	U_{11}	U_{12}	U_{13}	Weight
U_{11}	1	1/6	1/2	0.11
U_{12}	6	1	3	0.67
U_{13}	2	1/3	1	0.22

Table 3: Judgment matrix table U_2.

Technological factors U_2	U_{21}	U_{22}	U_{23}	Weight
U_{21}	1	1/2	1	0.25
U_{22}	2	1	1	0.5
U_{23}	1	1	1	0.25

Table 4: Judgment matrix table U_3.

Human factors U_3	U_{31}	U_{32}	U_{33}	U_{34}	Weight
U_{31}	1	1	1/2	1/2	0.2
U_{32}	1	1	1/2	1/2	0.2
U_{33}	1	2	1	2	0.2
U_{34}	2	2	1/2	1	0.4

Table 5: RI values of average random consistency index.

n	RI
1	0
2	0
3	0.58
4	0.90
5	1.12
6	1.24
7	1.32
8	1.41
9	1.45

Table 6: Overall ranking of synthetic weights of evaluation indicators.

Impact factor	Total sorts	Weight W_i
Hard and soft interbed	1	0.406
Angle of bedding	2	0.133
Device structure	3	0.133
Anisotropy	4	0.067
Rig-up	5	0.066
Drilling tool weight	6	0.066
Drilling rate choice	7	0.052
Drilling method	8	0.026
Drilling parameter	9	0.026
WOB choice	10	0.025

the rock to the *L*8 limestone produces large deviations. The "soft–hard–soft" rock formation means that it is necessary to drill through the interface between hard rock and soft rock. When the angle of the encountered layer is less than the critical angle, the main force results in downward deflection.

(b) *When the Angle of the Encountered Layer is Greater Than the Critical Value*. When the angle of the encountered layer is greater than the critical value, Figures 7 and 8 show that there is an overall upward deflection, with a drilling deflection angle of 0–6° and an overall offset of 1–7.2 m (average of 4.1 m). The

(a) (b)

Figure 2: Inclination test site. (a) Drilling site at the early stage of treatment. (b) Drilling at the later stage of treatment.

Table 7: Drilling deviation.

Data classification	Proportion (%)
Vertex angle θ and azimuth angle α are unchanged	0.5
Vertex angle θ changes; azimuth angle α is unchanged	10.9
Vertex angle θ and azimuth angle α both change	81.9
Apex angle θ remains unchanged; azimuth angle α changes	6.7

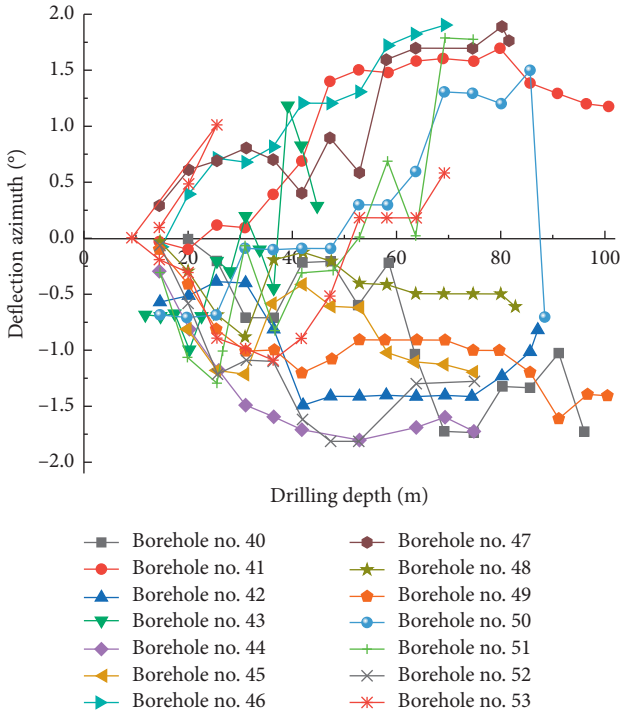

Figure 3: Azimuth change diagram.

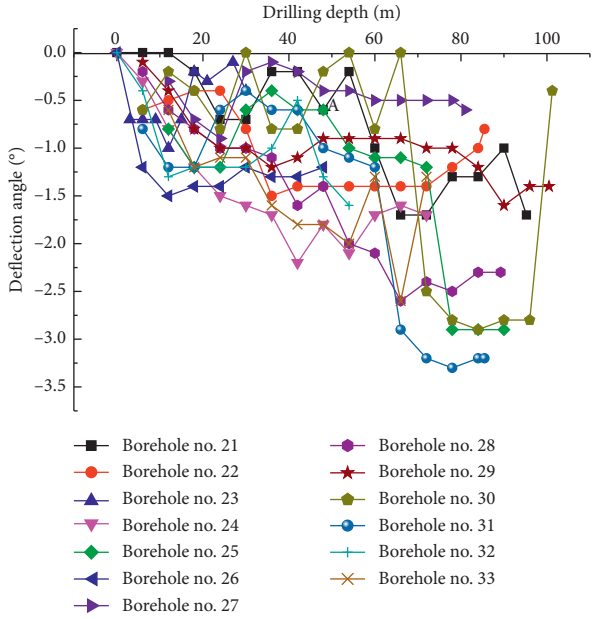

Figure 4: Change in the dip angle when the angle of encountered layer is less than the critical value.

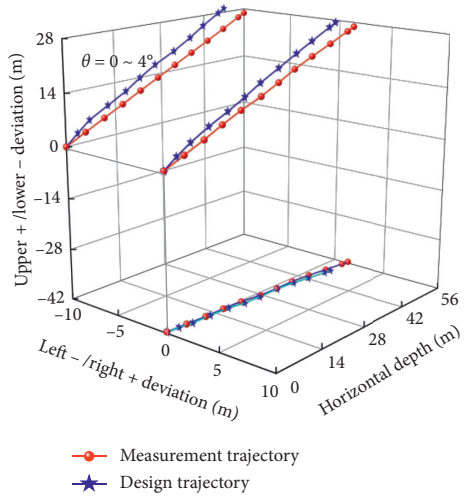

Figure 5: Borehole offset when the angle of encountered layer is less than the critical value.

offset in the vertical direction due to the angle of the layer being greater than the critical value grows as the borehole becomes deeper. Therefore, over the extent of the slanted borehole trajectory, the offset gradually increases.

The borehole deflection is compared with a geological model figure corresponding to *L*8 limestone in Figure 9. Sandy mudstone induces small deviations, whereas drilling through the *L*8 limestone produces significant deflections. When drilling through "soft–hard–soft" rock interfaces, if the angle of the encountered layer is greater than the critical angle, the resultant force is mainly towards the hard rock interface, and so the main deflection is upward.

4.3. Inclinometer Trajectory Fitting and Prediction. From the rock coring drilling trajectory data collected in this study, a borehole trajectory nonlinear regression equation was constructed. A scatter plot of the trajectories is shown in Figure 10.

The final fitting results were obtained as follows:

$$\theta = (-2.35484 \pm 0.89571) \cdot e^{(-L/(3.53216 \pm 3.00351))} + (2.13432 \pm 0.2785). \quad (10)$$

Comprehensive analysis, theoretical analysis, and the prediction model exhibit good consistency. Therefore, the proposed approach can adequately represent the deflection in the process of drilling, allowing adjustable control to be implemented during the drilling process.

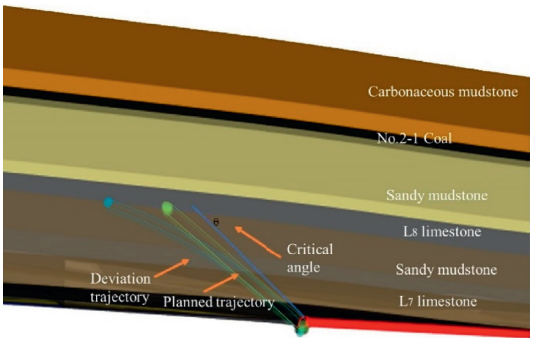

Figure 6: Comparison of stratigraphic restoration.

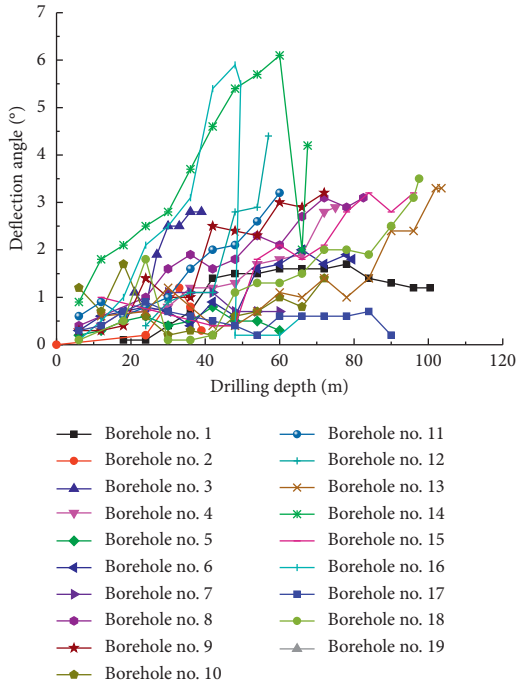

Figure 7: Change in the dip angle when the angle of encountered layer is greater than the critical value.

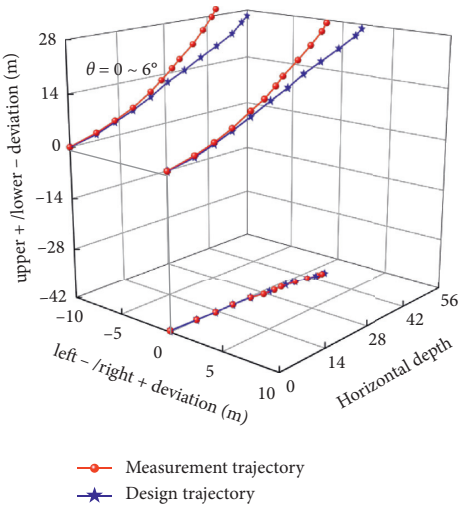

Figure 8: Borehole offset when the angle of encountered layer is greater than the critical value.

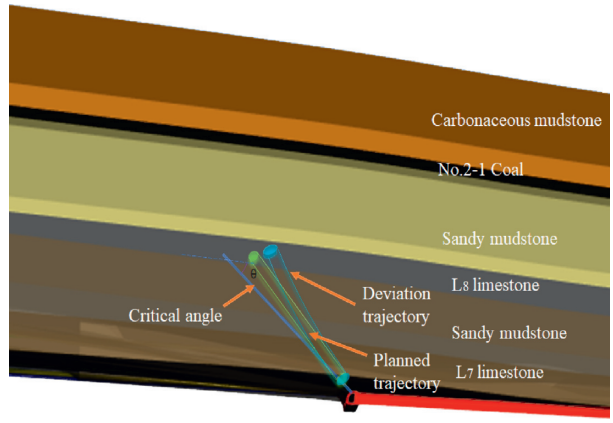

Figure 9: Comparison of stratigraphic restoration.

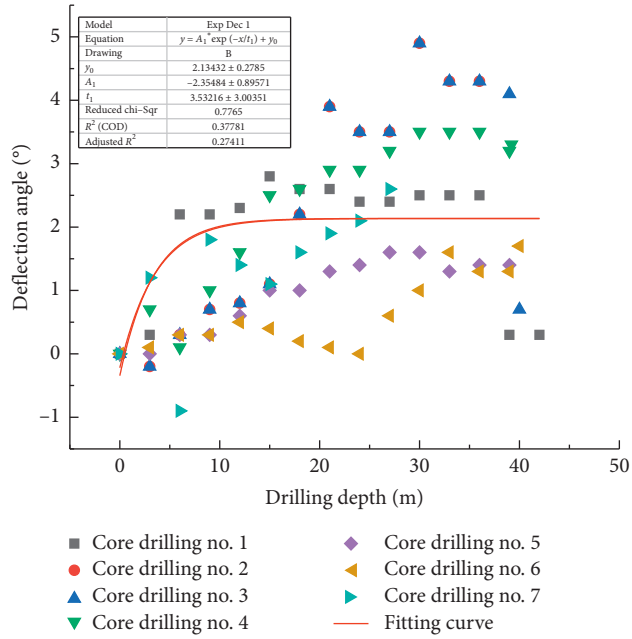

Figure 10: Scatter plot.

5. Conclusions

For the problem of gas drainage borehole deflection, an AHP model has been established to rank the weights of various influencing factors, and the analysis has been combined with a drilling model and engineering examples. The primary conclusions from this study are as follows:

(1) The soft and hard interlayers are critical factors influencing gas drainage borehole deflection.

(2) In the process of drilling, when there are soft and hard interlayers at the interface, the critical drilling inclination angle ranges from 25 to 35°. When the dip angle is greater than the critical angle, the inclination angle generally moves upward with a deflection angle of 0–6°, and the borehole deflection occurs mainly in the rock layer interface. When the angle of the encountered layer is less than the critical value, the overall drilling angle is deflected downward, and the skew angle is from 0 to 4°.

(3) The theoretical model and field data for predicting the trajectory curve are consistent, enabling preliminary control of the drilling process. This provides a new way of thinking for borehole deflection governance.

Data Availability

All data, models, or code generated or used during the study is available from the corresponding author upon request.

Conflicts of Interest

The authors declare that they have no conflicts of interest.

Acknowledgments

This work was financially supported by the National Natural Science Foundation of China (52074120), Program for Science & Technology Innovation Talents in Universities of Henan Province (19HASTIT047), and Science and Technology Project of Henan Province (182102310012). This support is gratefully acknowledged.

References

[1] X. Li, Z. Cao, and Y. Xu, "Characteristics and trends of coal mine safety development," *Energy Sources, Part A: Recovery, Utilization, and Environmental Effects*, pp. 1–19, 2020.

[2] Q. Zou, H. Liu, Y. Zhang, Q. Li, J. Fu, and Q. Hu, "Rationality evaluation of production deployment of outburst-prone coal mines: a case study of nantong coal mine in Chongqing, China," *Safety Science*, vol. 122, Article ID 104515, 2020.

[3] J. Dennis, "Black . Review of coal and gas outburst in Australian underground coal mines," *International Journal of Mining Science and Technology*, vol. 29, no. 6, pp. 815–824, 2019.

[4] C. Fan, S. Li, and M. Luo, "Coal and gas outburst dynamic system," *International Journal of Mining Science and Technology*, vol. 27, no. 1, pp. 49–55, 2017.

[5] J. Geng, X. Jiang, and N. Wen, "Regression analysis of major parameters affecting the intensity of coal and gas outbursts in laboratory," *International Journal of Mining Science and Technology*, vol. 27, no. 2, pp. 327–332, 2017.

[6] F. Wu, H. Zhang, Q. Zou, C. Li, J. Chen, and R. Gao, "Viscoelastic-plastic damage creep model for salt rock based on fractional derivative theory," *Mechanics of Materials*, vol. 150, no. 103600, 2020.

[7] F. Wu, J. Liu, Q. Zou, C. Li, J. Chen, and R. Gao, "A triaxial creep model for salt rocks based on variable-order fractional derivative," *Mechanics of Time-dependent Materials*, vol. 25, pp. 101–118, 2020.

[8] B. Zhang, H. Sun, Y. Liang, K. Wang, and Q. Zou, "Characterization and quantification of mining-induced fractures in overlying strata: implications for coalbed methane drainage," *Natural Resources Research*, vol. 29, no. 4, 2019.

[9] D. Rudakov and V. Sobolev, "A mathematical model of gas flow during coal outburst initiation," *International Journal of Mining Science and Technology*, vol. 29, no. 5, pp. 791–796, 2019.

[10] J. Ou, M. Liu, and C. Zhang, "Determination of indices and critical values of gas parameters of the first gas outburst in a coal seam of the Xieqiao Mine," *International Journal of Mining Science and Technology*, vol. 22, no. 1, pp. 29–93, 2012.

[11] Q. Zou, L. Han, Z. Cheng, T. Zhang, and B. Lin, "Effect of slot inclination angle and borehole-slot ratio on mechanical property of pre-cracked coal: implications for ECBM recovery using hydraulic slotting," *Natural Resources Research*, vol. 29, pp. 1705–1729, 2020.

[12] T. Liu, B. Lin, X. Fu et al., "Experimental study on gas diffusion dynamics in fractured coal: a better understanding of gas migration in in-situ coal seam," *Energy*, vol. 195, Article ID 117005, 2020.

[13] T. Liu, S. Liu, B. Lin, X. Fu et al., "Stress response during in-situ gas depletion and its impact on permeability and stability of CBM reservoir," *Fuel*, vol. 266, Article ID 117083, 2020.

[14] Q. Zou, B. Lin, C. Zheng et al., "Novel integrated techniques of drilling–slotting–separation-sealing for enhanced coal bed methane recovery in underground coal mines," *Journal of Natural Gas Science and Engineering*, vol. 26, pp. 960–973, 2015.

[15] H. Jiang and Y. Luo, "Development of a roof bolter drilling control process to reduce the generation of respirable dust," *International Journal of Coal Science & Technology*, vol. 8, no. 2, pp. 199–204, 2021.

[16] H. Gao, Qi Wang, and B. Jiang, "Relationship between rock uniaxial compressive strength and digital core drilling parameters and its forecast method," *International Journal of Coal Science & Technology*, 2021.

[17] Y. Hui, H. Jia, and S. Liu, "Macro and micro grouting process and the influence mechanism of cracks in soft coal seam," *International Journal of Coal Science & Technology*, 2021.

[18] Z. F. Wang, T. Hen, F. M. An et al., "Experimental research of gas drainage in extremely short-distance over-lying adjacent seam," *Journal of Henan Polytechnic University(Natural Science)*, vol. 36, no. 1, pp. 12–16, 2017.

[19] G. Y. Li and Y. P. Xu, "Gas drainage technology with super long high directional drilling in goaf roof," *Coal Engineering*, vol. 49, no. 8, pp. 88–91, 2017.

[20] D. Gao, Z. Dong, and H. Zhang, "On appropriately matching the bottomborehole pendulum assembly with the anisotropic drill bit, to control the borehole-deviation," *Computer Modeling in Engineering and Sciences*, vol. 89, no. 2, pp. 111–122, 2012.

[21] W. Wang, H. Zhang, N. Li et al., "The dynamic deviation control mechanism of the prebent pendulum BHA in air drilling," *Journal of Petroleum Science and Engineering*, 2019.

[22] D. Gao and D. Zheng, "Study of a mechanism for well deviation in air drilling and its control," *Petroleum Science and Technology*, vol. 29, no. 4, pp. 358–365, 2011.

[23] R. H. Morin and R. H. Wilkens, "Structure and stress state of Hawaiian island basalts penetrated by the Hawaii Scientific Drilling Project deep core borehole," *Journal of Geophysical Research: Solid Earth*, vol. 110, no. 404, pp. 1–8, 2005.

[24] Y. Chen, J. Fu, T. Ma et al., "Numerical modeling of dynamic behavior and steering ability of a bottom borehole assembly with a bent-housing positive displacement motor under rotary drilling conditions," *Energies*, vol. 11, no. 10, 2018.

[25] C. Liu, F. Zhou, and K. Yang, "Failure analysis of borehole liners in soft coal seam for gas drainage," *Engineering Failure Analysis*, vol. 42, pp. 274–283, 2014.

[26] F. Gao, Z. Zhang, Y. Gao et al., "Risk assessment model of rockburst based on blind number theory," *Journal of China Coal Society*, vol. 35, no. S1, pp. 28–32, 2010.

[27] X. Wang and D. Huo, "Application of fuzzy comprehensive evaluation method in coal mine safety evaluation," *China Mining Industry*, vol. 4, no. 5, pp. 75–78, 2008.

[28] X. S. Guo and N. Kapucu, "Assessing social vulnerability to earthquake disaster using rough analytic hierarchy process method: a case study of Hanzhong City, China," *Safety Science*, vol. 125, Article ID 104625, 2020.

[29] A. Petruni, E. Giagloglou, E. Douglas, J. Geng, M. C. Leva, and M. Demichela, "Applying Analytic Hierarchy Process (AHP) to choose a human factors technique: choosing the suitable Human Reliability Analysis technique for the automotive industry," *Safety Science*, vol. 119, pp. 229–239, 2019.

[30] L. I. Ning, L. Wang, and M. Jia, "Fuzzy comprehensive evaluation of six mine systems based on analytic hierarchy process," *Journal of Central South University: Science and Technology*, vol. 46, no. 2, pp. 631–637, 2015.